



Network of European Research Infrastructures for Earthquake Risk Assessment and Mitigation

Report

Updating building capacity during an earthquake sequence

Activity:	<i>Real-time seismic risk assessment and decision support</i>
Activity number:	<i>WP14, Task 14.2</i>
Deliverable:	<i>Updating building capacity during an earthquake sequence</i>
Deliverable number:	<i>D14.2, Version 12.12</i>
Responsible activity leader:	<i>J. Douglas Zechar</i>
Responsible participant:	<i>ETH Zurich</i>
Author:	<i>B. Borzi</i>



TABLE OF CONTENTS

1	Introduction	5
2	Literature review	7
2.1	Methods relevant for SP-BELA approach	7
3	Overview of large scale vulnerability methods adopted in WP 14.....	13
3.1	Overview of SP-BELA method	13
3.1.1	RC buildings.....	13
3.1.2	Masonry buildings	20
4	Proposed method to account for progressive damage.....	26
4.1	Modifications of SP-BELA to account for progressive damage	26
4.1.1	Application of the SP-BELA method accounting for progressive damage	29
5	Closure and further developments	31

1 INTRODUCTION

The problem of assessing the capacity of a typical existing structure to sustain the effects of an earthquake has always represented a big challenge for structural engineers, in particular in the past few decades, when specific and detailed seismic codes have been developed and applied in the vast majority of the countries of the world. Hence the problem in terms of seismic performance is related to existing buildings, while the new designed one are expected to have adequate structural capacity. Several methods have been proposed in the past to fulfil the purpose on large scale structural assessment. Such methods can be grouped in “analytical methods”, “empirical methods” and “hybrid methods” that are a combination of the first two.

Analytical methods for the assessment of the seismic vulnerability of buildings have only recently become feasible due to a combination of advancements in the field of seismic hazard assessment and structural response analysis. In the past, empirical methods based on the observed damage data of buildings in terms of macroseismic intensity were popular because they allowed the data to be convolved with seismic hazard maps, which were also in terms of macroseismic intensity. However, recent developments in probabilistic seismic hazard assessment have led to the production of seismic hazard maps in terms of peak ground acceleration (PGA) and spectral ordinates, allowing methods which correlate the damage of the building stock to these input parameters to be proposed.

Analytical vulnerability assessment approaches tend to feature, with respect to empirical methods, slightly more detailed and transparent vulnerability assessment algorithms with direct physical meaning, that not only allow detailed sensitivity studies to be undertaken, but also cater for more straightforward calibration to various characteristics of building stock and hazard. Such characteristics place this type of loss assessment methods in an ideal position for employment in parametric studies that aim at the definition/calibration of urban planning, retrofitting, insurance and other similar policies or initiatives.

The flowchart presented in Figure 1.1 shows the components generally included in the analytical evaluation of vulnerability curves for the seismic assessment of buildings. One of the main differences between analytical methods arises in the computational modelling of the structural behaviour and in particular the procedure used to define the nonlinear response of the structure to a given ground motion input.

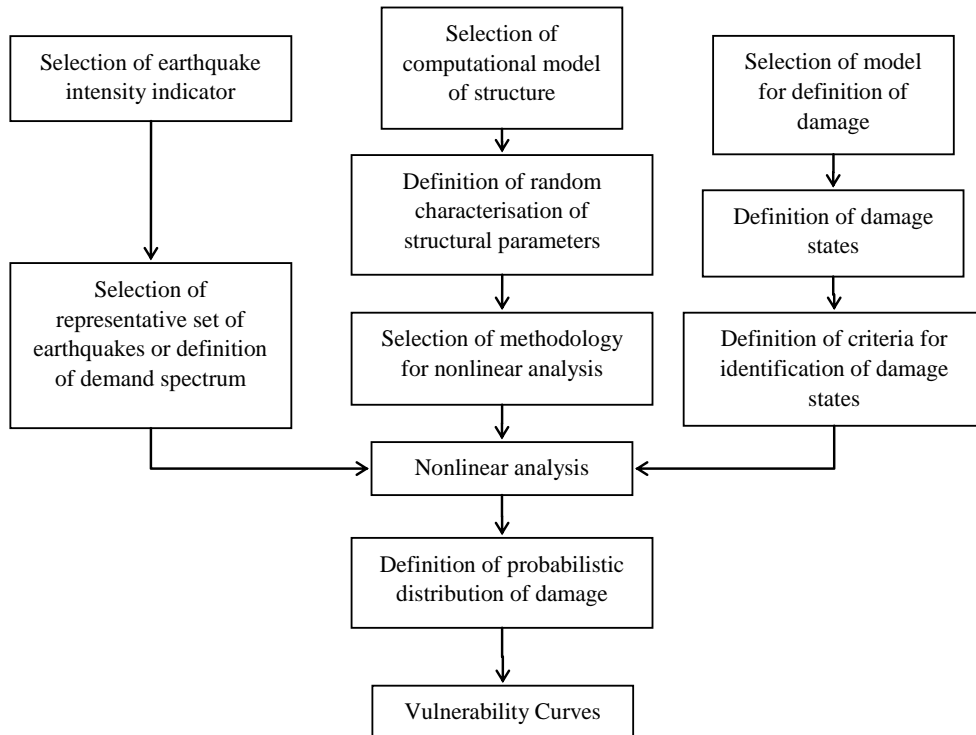


Figure 1.1. Flowchart to describe the components of the calculation of analytical vulnerability curves (adapted from Dumova-Jovanoska, 2004).

Many of the original procedures aimed to the large scale vulnerability assessment are based on the post-processing of the results of nonlinear analyses on a detailed model of the structure (e.g. Singhal and Kiremidjian, 1996; Masi, 2004; Rota, 2010), which has to be implemented in a finite element code, and this can be a strong limitation for several reasons. First of all, nonlinear analyses can be very time consuming. Moreover, finite element codes are often expensive and require very skilled and trained users to be utilized as a reliable tool. Finally, the variability of the structural capacity is not well represented because only some of the model parameters are random variables and the others correspond to the deterministic characteristic of the prototype buildings (e.g., the building geometry is usually deterministic and the material resistance is random).

The mechanics based methods adopted for the purposes of this work are:

- a methodology published in the technical literature with the acronym SP-BELA (Simplified Push Over Based Earthquake Loss Assessment). Such methodology has been applied for the large scale vulnerability assessment and to produce fragility curves that mathematically represent vulnerability of RC, masonry and RC pre-cast buildings (Borzi et al., 2007; Borzi et al., 2008; Bolognini et al., 2008). The methods rely on a simplified model of the structure. The seismic performance is then defined through a simplified pushover analysis. When using SP-BELA, the building stock is classified in different structural typologies and to each typology a prototype structure is associated. This structure is used to obtain with a Monte Carlo generation a population of buildings whose structural performance is defined through a simplified pushover analyses. Through a comparison between capacity and demand, both expressed in terms of displacements that are well correlated to damage, in a probabilistic framework, fragility curves can be computed. For the purpose of this deliverable no fragility curves are computed and SP-BELA is adopted up to the definition of pushover curves. This choice leads to several advantages that can be seen better later in the current document;

Another important aspect of the seismic assessment of existing buildings is the effect of progressive damage. In some cases, a specific seismic event is characterized by a main shock of strong intensity that is followed, in the next hours or days, by one or more aftershocks. Even if the intensity of the aftershock alone would not be able to cause any serious damage to some of the structures, considering that the damage, which has been produced by the main shock, has not been repaired and that the structure has not been retrofitted, the subsequent seismic event can cause, in some structures, an heavy level of damage and, in some cases, the structure itself can collapse. Moreover, sometimes the history of the seismic events, that a particular construction has undergone, is unknown, as well as the eventual retrofitting or repair interventions that have been carried out on it. For all these reasons, the development of a procedure to evaluate the capacity of an existing building and to predict, with good approximation, its structural response under the effect of progressive damage is of crucial importance. This procedure should be simple and quick to apply, it should require no finite element analyses and it should need the smallest possible level of detail in the knowledge of the building characteristics. As regards the information about the damaging events, a good and simple procedure should not require any original record but only a basic knowledge of the seismicity of the site where the construction is located, in the form of a spectrum.

The purpose of this work is to develop a building assessment methodology which presents all the aforementioned characteristics. Hence, the large scale vulnerability assessment methodology will be expanded to account for progressive damage.

In this report chapter 2 is about a literature review of the methods developed in the past to take into account the progressive damage while in chapter 3 there is an overview of the large scale vulnerability methods adopted in WP14 and chapter 4 illustrates the proposed method to account for progressive damage. Finally, chapter 5 contains the conclusions and the future developments.

2 LITERATURE REVIEW

The following paragraphs summarise the literature of the methods that account for progressive damage. The methods are grouped as a function of the vulnerability assessment method to which they can be associated.

2.1 METHODS RELEVANT FOR SP-BELA APPROACH

Since SP-BELA describes the structural performance through a pushover curve, it becomes paramount to account for progressive damage adopting methods that modify the pushover curve parameters like initial stiffness, base shear resistance and displacement capacity. This approach was followed by FEMA research groups that had, as major inspiration, to provide professionals with practical guide on how to take into account pre-existing damage on a structure. In 1998 two documents were published on the evaluation of earthquake-damaged concrete and masonry wall buildings: a basic procedure manual (FEMA306, 1998) and a technical resource manual (FEMA307, 1998).

The damage evaluation procedures illustrated in FEMA306 are performance-based and a performance level typically is defined by a particular damage state for a building. The performance levels defined in a previous FEMA document (FEMA273, 1997) are: collapse prevention, life safety, and immediate occupancy. Hazards associated with future hypothetical earthquakes are usually defined in terms of ground shaking intensity with a certain likelihood of being exceeded over a defined time period or in terms of a characteristic earthquake likely to occur on a given fault. The combination of a performance level and a hazard defines a performance objective. The damage evaluation begins with the selection of an appropriate performance objective. The performance objective serves as a benchmark for measuring the difference between the anticipated performance of the building in its damaged and pre-event states, that is, relative to performance analysis.

For a given global displacement of a structure subject to a given lateral load pattern, there is an associated deformation of each structural component of the building. Since inelastic deformation indicates component damage, the maximum global displacement to occur during an earthquake defines a structural damage state for the building in terms of inelastic deformations for each of its components. The capacity of the structure is represented by the maximum global displacement, d_c , at which the damage of the weakest component is at the limit of exceeding the tolerable limit for a specific performance level.

The analysis methodologies also include techniques to estimate the maximum global displacement demand, d_d , for a specific earthquake ground motion. The ratio of the displacement capacity, d_c , of the building for a specific performance level to the displacement demand, d_d , for a specific hazard is a measure of the degree to which the building meets the performance objective. If the ratio is less than 1.0 the performance objective is not met. If it is equal to one the objective is just met. If it is greater than 1.0, the performance exceeds the objective.

Damage caused by an earthquake can affect the ability of a structure to meet the performance objectives for future earthquakes in two fundamental ways. First, the damage may cause the displacement demand for the future event, d'_d , to differ from that for the pre-event structure, d_d . This is due to changes in the global stiffness, strength, and damping of the structure, which in turn affects the maximum dynamic response of the structure by changing its global stiffness, strength, and damping. Also, the displacement capacity of the damaged structure, d'_c , may differ from that of the pre-event structure, d_c . Damage to the structural components can change the magnitude of acceptable deformation for a component in future earthquakes.

The analysis procedure described further on uses the change in the ability of the damaged building to meet the performance objectives in future earthquakes to measure the effects of the damage.

The approach proposed in FEMA consists of a quantitative procedure that uses nonlinear static techniques to estimate the performance of the building in future events in both its pre-event and damaged states. This procedure requires the selection of one or more performance objectives for the building as already discussed. The analysis compares the degree to which the pre-event and damaged buildings meet the specified objective.

The nonlinear static procedures estimate the maximum global displacement of a structure due to shaking at its base. These procedures are easier to implement and understand than nonlinear dynamic time history analyses, but they are relatively new and need further development.

The basic steps for using the procedure to measure the effect of damage caused by the damaging ground motion on future performance are outlined as follows:

1. using the properties (strength, stiffness, energy dissipation) of all of the lateral-force-resisting components and elements of the pre-event structure, formulate a capacity curve relating global lateral force to global displacement;
2. determine the global displacement limit, d_c , at which the pre-event structure would just reach the performance level specified for the performance objective under consideration;
3. for the specified performance ground motion, determine the hypothetical maximum displacement for the pre-event structure, d_d . The ratio of d_c to d_d indicates the degree to which the pre-event structure satisfies the specified performance objective;
4. using the results of the investigation of the effects of the damaging ground motion, modify the component force-deformation relationships using the Component Damage Classification Guides in FEMA (FEMA306, 1998) or through direct investigation. Using the revised component properties, reformulate the capacity curve for the damaged building and repeat steps 2 and 3 to determine d'_c and d'_d . The ratio of d'_c to d'_d indicates the degree to which the damaged structure satisfies the specified performance objective;

5. if the ratio of d'_c to d'_d is the same, or nearly the same, as the ratio of d_c to d_d , the damage caused by the damaging ground motion has not significantly degraded future performance for the performance objective under consideration;
6. if the ratio d'_c to d'_d is less than the ratio of d_c to d_d , the effects of the damage caused by the damaging ground motion has diminished the future performance characteristics of the structure. Develop hypothetical actions to restore or augment element and component properties so that the ratio d^*_c to d^*_d (where the * designates the restored condition) is the same, or nearly the same, as the ratio of d_c to d_d .

The global displacement performance limits are a function of the acceptability of the deformation of the individual components of the structure as it is subjected to appropriate vertical loads and to a monotonically increasing static lateral load distributed to each floor and roof level in an assumed pattern. The plot of the total lateral load parameter versus global displacement parameter represents the capacity curve for the building for the assumed load pattern. Thus, the capacity curve is characteristic of the global assembly of individual components and the assumed load pattern. The current provisions of FEMA (1997) limit global displacements for the performance level under consideration (e.g., Immediate Occupancy, Life Safety, Collapse Prevention) to that at which any single component reaches its acceptability limit (see Figure 2.1).

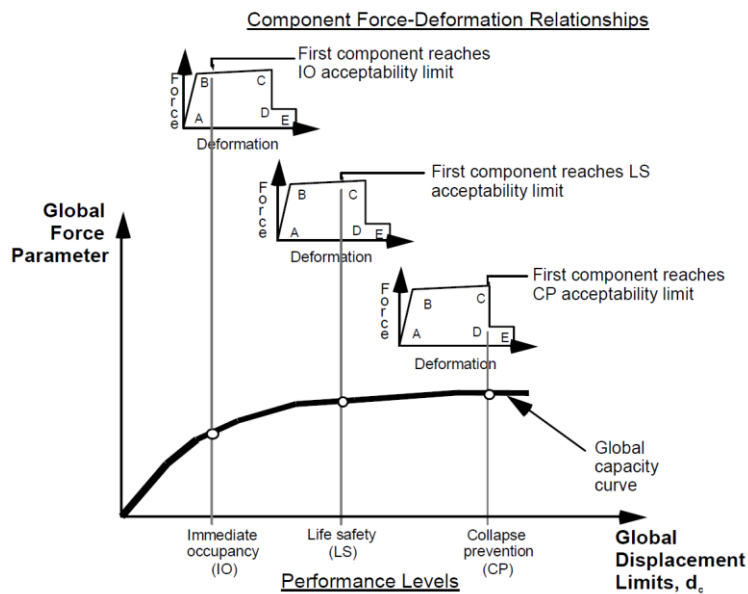


Figure 2.1. Global Displacement Limits and Component Acceptability used in FEMA (FEMA306, 1998).

The effects of damage on component behaviour are modelled as shown generically in Figure 2.2.

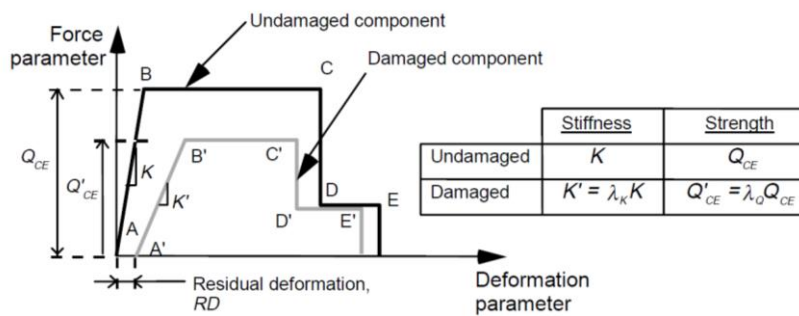


Figure 2.2. Component modelling criteria (FEMA306, 1998).

Acceptability criteria for components are illustrated in Figure 2.3.

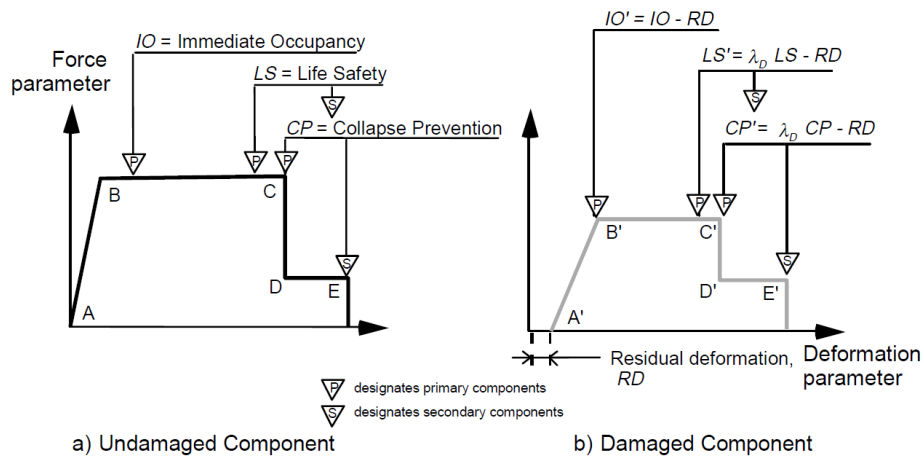


Figure 2.3. Component acceptability criteria (FEMA306, 1998).

The factors used to modify component properties are defined as follows:

- λ_K : modification factor for idealized component force-deformation curve accounting for change in effective initial stiffness resulting from earthquake damage;
- λ_Q : modification factor for idealized component force-deformation curve accounting for change in expected strength resulting from earthquake damage;
- λ_D : modification factor applied to component deformation acceptability limits accounting for earthquake damage;
- RD: absolute value of the residual deformation in a structural component, resulting from earthquake damage.

The values of the modification factors depend on the behaviour and the severity of damage of the individual component. They are tabulated in the Component Guides in FEMA 306 (1998).

The modification factors proposed in FEMA 306 have been used by Polese et al. (2012) for deriving damage-dependent vulnerability curves. In particular, Polese et al. (2012) have developed a method to define the seismic behaviour of buildings as a function of their REsidual Capacity (REC), which is the measure of seismic capacity compromised by the damage. In the framework of a mechanically based vulnerability method, the REC may be evaluated from pushover curves obtained for the structure in different damage conditions.

The basic steps followed by Polese et al. (2012) to determine the variation in building vulnerability from undamaged to collapse limit condition are (see the flowchart in Figure 2.4 for frame structures):

- **Building model (Step 1):** global capacity parameters may be determined with pushover analysis performed on a lumped plasticity model. For RC frame buildings, element flexural behavior is conveniently characterized by a bilinear moment–rotation plastic hinge, described by yielding (M_y and θ_y) and ultimate (M_u and θ_u) moment and rotation. The moments M_y and M_u can be determined by moment–curvature analyses for the element’s sections;

- **Pushover analysis for the undamaged structure and evaluation of damage limit condition (Step 2):** the analysis procedure described in FEMA 306 (1998) is intended to assess the performance of buildings that have actually been damaged by a seismic event. The damage level of the structural elements is assessed by local inspection of the structure. On the basis of the type of elements, the observed behaviour (e.g. pure flexural, flexure-shear, sliding shear, etc.), and the severity of damage, suitable factors to modify plastic hinge properties in the models are suggested. In the study of Polese et al. (2012), three damage limit conditions have been adopted such as: D1, limited damage; D2, moderate damage and D3, high damage;
- **Model for damaged buildings (Step 3):** for each of the global damage levels considered (D_k with $k = 1, 2, 3$), a modified nonlinear model is built. In particular, according to the local damage level attained by the structural elements in the deformed shape at D_k , the corresponding plastic hinges are modified with a suitable variation in the relative stiffness ($K' = \lambda_k K$), strength ($M_y' = \lambda_Q M_y$) and plastic rotation capacity ($a' = a - a_d = a - (\theta_y' - \theta_y) - RD = a - (\theta_y (\lambda_Q / \lambda_k - 1) - RD)$), with λ the stiffness/strength modification factors and RD the residual drift of the element;
- **Pushover analysis for damaged buildings (Step 4):** nonlinear static analysis of the modified damaged models. As a function of the number of elements involved in the collapse mechanism and of their damage, the new pushover curve may differ significantly from the original one;
- **Evaluation of REC (Step 5):** the residual capacity REC_{Sa} is defined, for each global damage state D_k , as the spectral acceleration at the equivalent vibration period T_{eq} that leads the building to collapse. In other words, it is the elastic spectral acceleration corresponding to the maximum allowable capacity of the equivalent SDOF. The method adopted in Polese et al. (2012) to find the demand–intensity relationship for the structures is the incremental N2 method (IN2) (Dolsek and Fajfar, 2004). Moreover, since the parameters adopted in large scale vulnerability assessment to measure the input motion severity is the peak ground acceleration PGA, a spectral shape is adopted to find the PGA corresponding to the acceleration spectral ordinate;
- **Damage-dependent collapse vulnerability curves (Step 6):** following the steps between 1 and 5 vulnerability curves for damaged buildings have been computed.

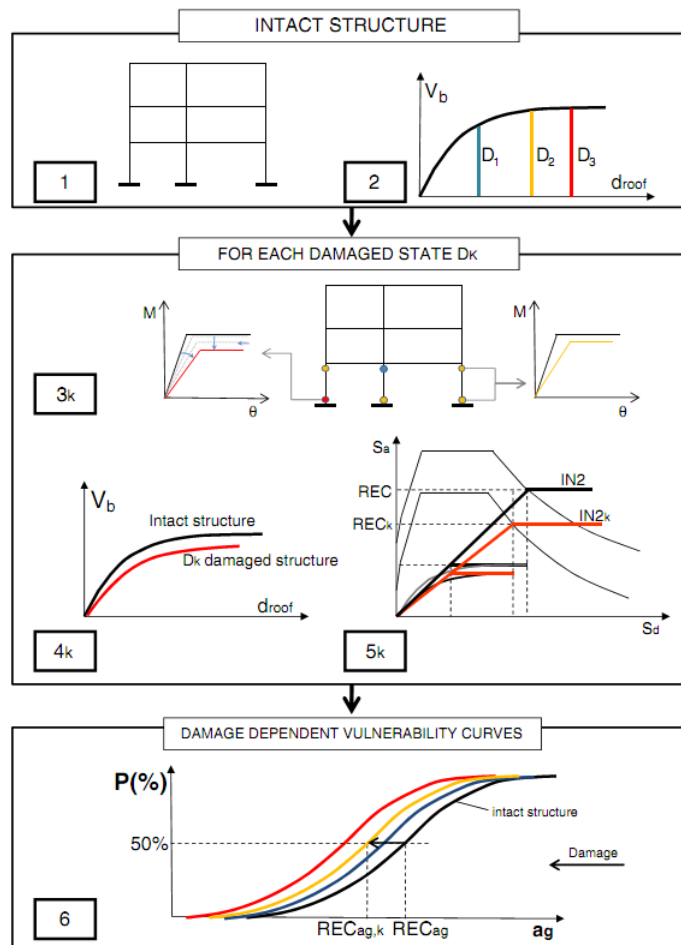


Figure 2.4. Flowchart of method proposed by Polese et al (2012 for RC frame buildings.

The modification factors (λ) and the RD residual drift were computed by Polese et al (2012) on the basis of experimental cyclic tests performed on RC full-scale columns. Figure 2.5a shows that λ_k decreases with an almost hyperbolic trend as the column drift increases. Degradation of column strength λ_Q , is reported in Figure 2.5b. For a given θ/θ_y , the experimental member strength degradation was computed as the ratio between the maximum horizontal force recorded at θ and the experimental peak force recorded during the test. Figure 2.5b shows a significant strength degradation for $\theta/\theta_y > 3$. Finally, the RD/ θ_y ratio is represented in Figure 2.5c as a function of θ/θ_y . The RD was computed as the lateral drift of the column corresponding to a force equal to zero, and start to be significant for $\theta/\theta_y > 1$.

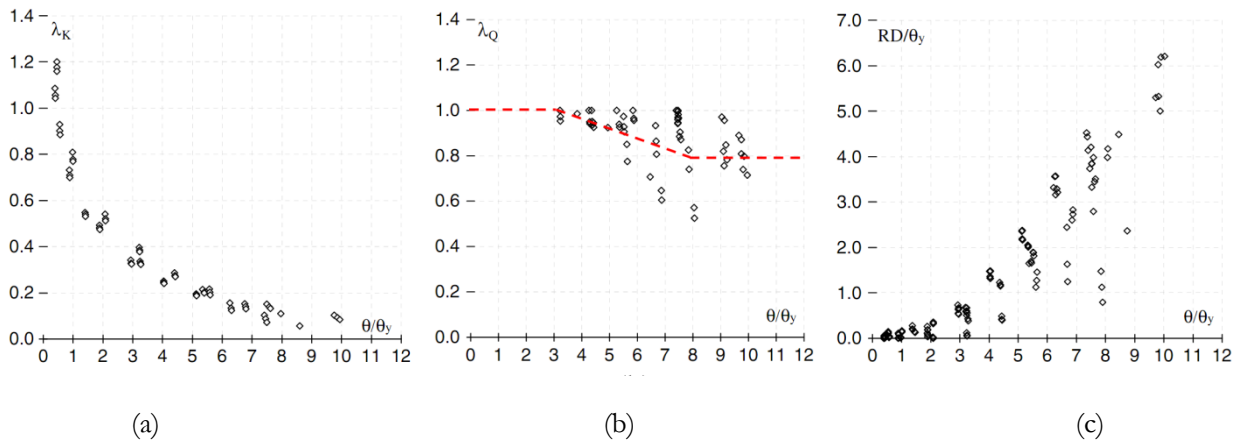


Figure 2.5. Modification factors: (a) relative stiffness, (b) strength, (c) residual drift RD.

3 OVERVIEW OF LARGE SCALE VULNERABILITY METHODS ADOPTED IN WP 14

3.1 OVERVIEW OF SP-BELA METHOD

A description of how SP-BELA computes the capacity for RC and masonry buildings will be given.

3.1.1 RC buildings

In order to compute capacity curves SP-BELA makes use of a simplified pushover methodology that can be employed in the assessment of a large number of buildings with reasonable computational effort. Within such framework, a three-linear curve is used, which effectively means that in order to define the pushover curve, only the collapse multiplier (λ which represents the ratio between base shear force and seismic weight) and the displacement capacity need to be defined (see Figure 3.1).

The control points on the curve correspond to three selected limit conditions such as: light damage, severe damage and collapse that need to be numerically identified. The drop of shear resistance observed in the post elastic branch is due to the collapse of infill wall. It is assumed that the infill walls collapse when the frame evolves in non linear branch and that the contribution of the infill wall to the lateral resistance is exhausted before the severe damage limit condition is achieved.

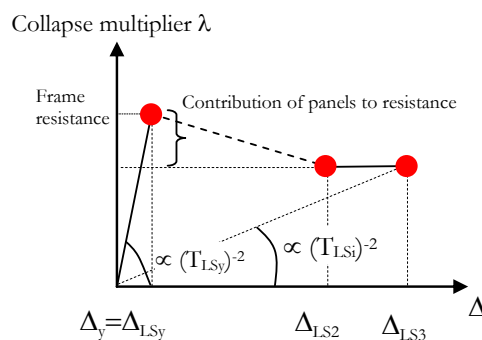


Figure 3.1. SP-BELA capacity curve.

In SP-BELA, the capacity curve is calculated for a prototype building (see Figure 3.2 and Figure 3.3). Other studies make reference to similar structural layout (e.g. Masi, 2004; Cosenza et al., 2005). Such buildings have frequently frames only in one direction when designed without accounting for seismic loading. In the weak direction, the frame effect is guaranteed by the edge beams and by the floor slabs alone. An effective width of the floor slab can be calculated assuming, for instance:

$$L_{col} = 4s + B_C \tag{3.1}$$

where L_{col} is the effective width of the floor slab, s is the floor slab thickness and B_C is the column dimension. Equation 3.1 expresses a definition of the equivalent width of floor slabs built according to typical construction practice in Mediterranean regions. These slabs are typically formed with light blocks separated by either cast-in-place or pre-cast RC ribs, and then a reinforced slab is cast on top.

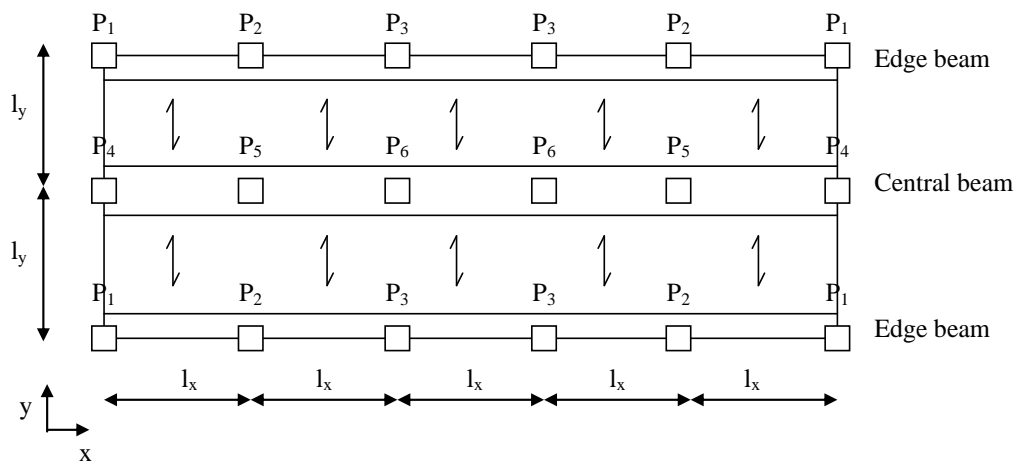


Figure 3.2. Plan view of the RC frame building assumed as representative of the building structural type.

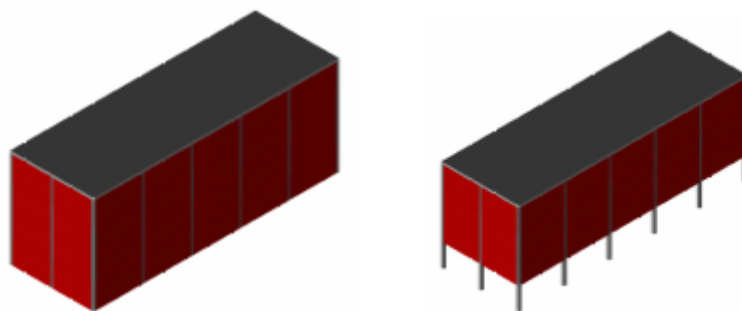


Figure 3.3. Infill panel distribution: regular (left) and irregular/pilotis (right).

Definition of collapse multiplier λ

In order to define the distribution of structural bending moments and shear forces in the elements of the frame, the seismic loads have been assumed to correspond to horizontal forces linearly distributed along the height, noting however that different distributions may be easily assumed, when relevant (e.g. for taller buildings where the effects of higher modes become important). The procedure, which inspires itself on the work of Priestley

and Calvi (1991), then calculates for each column of the frame the maximum value of shear that the column can withstand as the smallest of:

- the shear capacity of the column;
- the shear corresponding to the flexural capacity of the column;
- the shear corresponding to the flexural capacity of the beams supported by the column.

For the beams only the flexural collapse mechanism is taken into account, given that the beams tend to be less prone to shear failure than the columns since gravity load design typically features high shear forces in the beams and thus these elements have traditionally been provided with an adequate amount of shear reinforcement.

The checks conducted during the procedure to define the cause of failure in each column are illustrated in Figure 3.4, wherein the subscript R is for resistance and the subscripts C and B represent column and beam, respectively.

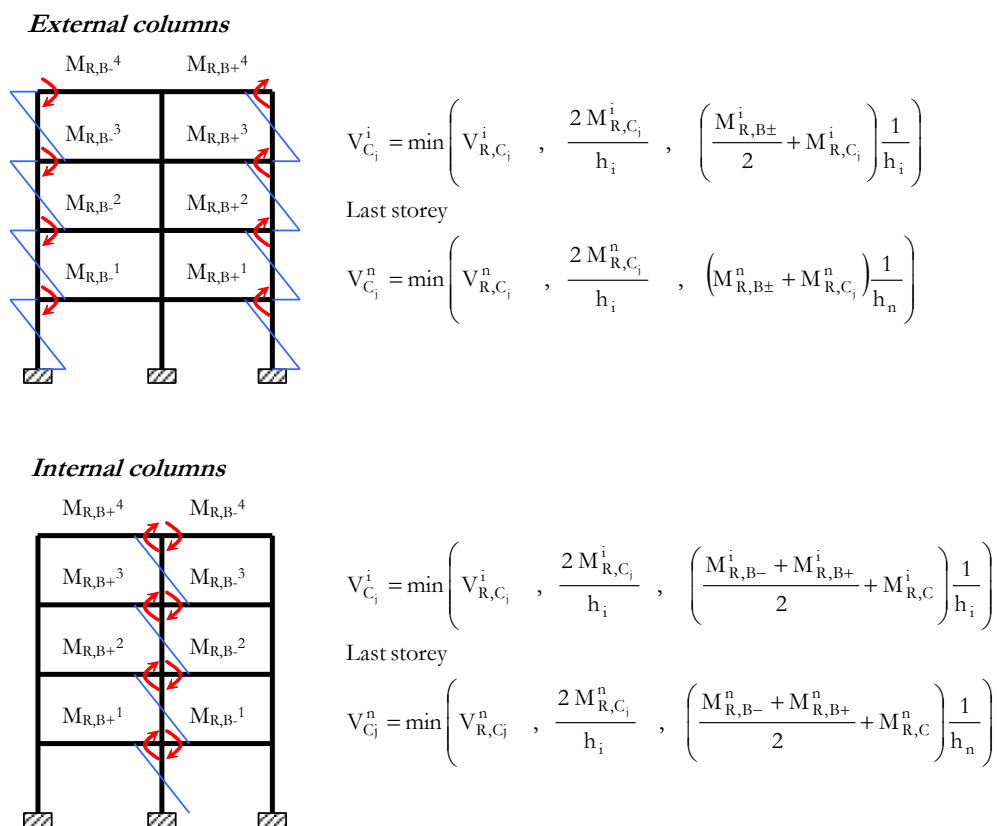


Figure 3.4. Maximum shear force that the columns in a frame can withstand accounting for (i) shear and flexural failure mechanism in columns and (ii) flexural failure mechanism in beams.

If the beams collapse before the columns, it is assumed that plastic hinges form at the base of the columns, as can be gathered from the equations in Figure 3.4. This is due to the fact that a mechanism can develop only when plastic hinges are activated in all columns at the same level. The equilibrium at the beam-column joints in the case of weak beams is shown in Figure 3.5.

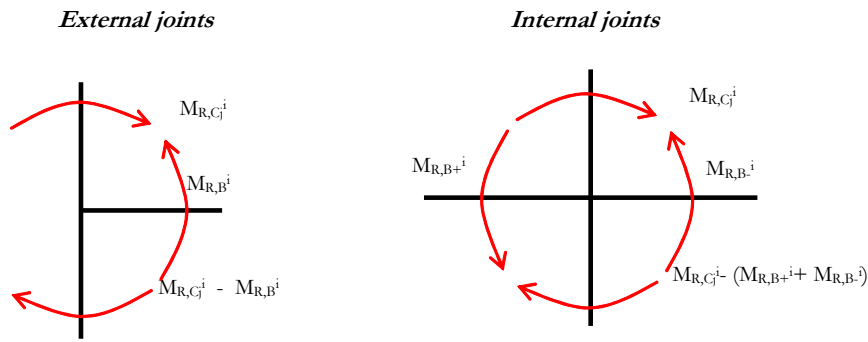


Figure 3.5. Equilibrium at the joint in the case of weak beams.

Once the shear capacity has been calculated for every storey, the collapse multiplier is defined by the following relationship:

$$\lambda^i = \frac{V_C^i \sum_{j=1}^n W_j z_j}{W_T \sum_{k=1}^n W_k z_k} \tag{3.2}$$

where W_T is the global building weight, W_i is the weight associated with floor i located at height z_i . The final collapse multiplier used to define the capacity curve will be the smallest λ^i .

Finally, in order to evaluate the collapse mechanism of the building the procedure uses the following criteria:

- if there is a shear failure mechanism detected in at least one column, the capacity curve will be interrupted at the lateral force that produces this failure. This choice is consistent with the fact that the shear failure mechanism is brittle and does not have associated dissipative capacity. Therefore, the structure cannot enter the nonlinear range;
- if after the development of plastic hinges in all beams, plastic hinges form in all columns at a certain level, a beam-sway collapse mechanism will be activated (Figure 3.6a);
- if all the columns within a certain storey fail in bending, than a column-sway collapse mechanism will be activated (Figure 3.6b).

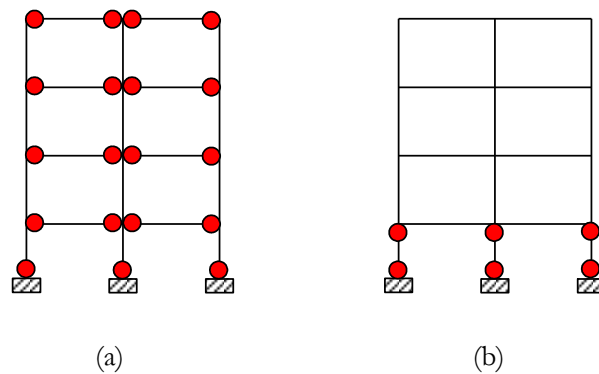


Figure 3.6. Possible collapse mechanisms for a frame (a) beam-sway collapse mechanism, (b) column-sway collapse mechanism.

There could be a situation in which at the storey corresponding to the smallest λ^i some of the columns are stronger than the beams, or vice versa. Therefore, it cannot be clearly identified whether a beam or a column-sway mechanism will be activated. The analyses undertaken to validate the SP-BELA procedure (Borzi, 2006) have shown that in such cases the collapse mechanism is an average between the column and the beam-sway.

The contribution to the frame resistance due to the infill panels is computed considering the panels acting in parallel. The infill panels are modelled through strut elements which have a thickness equal to the wall thickness and an equivalent width which is calculated according to the following relationship (Mainstone, 1971):

$$\frac{b_w}{d_w} = 0.2 \sin(2\vartheta) \left(\frac{E_w t_w h_w^3 \sin(2\vartheta)}{E_c I_p} \right)^{-0.1} \quad 3.3$$

where b_w is the equivalent width, d_w is the strut length, t_w is the panel thickness chosen as 250 mm in this application, ϑ is the angle that the strut forms with the horizontal line, h_w is the panel height, E_w is the elastic modulus of the panel, E_c is the elastic modulus of the concrete and I_p is the second moment of inertia of the columns. It is assumed that the panels have an influence on the lateral resistance of the building up to the yield limit state. Whereas, when the frames evolve into the nonlinear range, the panels are considered to collapse and, therefore, they no longer contribute to the base shear resistance.

Definition of displacement capacity

On the capacity curve, the displacement capacity can be related to damage conditions which are identifiable through Limit States (LS). As previously stated, three limit state conditions have been taken into account: light damage, significant damage and collapse. The light damage limit condition refers to the situation where the building can be used after the earthquake without the need for repair and/or strengthening. Beyond the limit condition of significant damage the building cannot be used after the earthquake without strengthening. Furthermore, this level of damage is such that it might not be economically advantageous to repair the building. If the collapse limit condition is achieved, the building becomes unsafe for its occupants as it is not capable of sustaining any further lateral force nor the gravity loads for which it has been designed.

To quantify whether a structural element achieves a limit condition the chord rotation in the columns of the storey where the collapse mechanism is activated is compared with limit rotation capacities. The influence of the panels is currently not considered in defining the displacement capacity on the pushover curve as the panels are often not perfectly in contact with the frames and they are assumed to play a role on the overall building performance only after the frames have already been deformed beyond their elastic limit. On the other hand, the panels are assumed to collapse before the frames reach the significant damage limit condition. The relationships adopted to numerically identify the displacement capacity on the pushover curves are:

- **Light damage limit state (LS1):** The rotation capacity is limited by the chord rotation corresponding to yielding Θ_y (Panagiotakos and Fardis, 2001; CEN, 2003):

$$\Theta_y = \phi_y \frac{L_V}{3} + 0.0013 \left(1 + 1.5 \frac{h}{L_V} \right) + 0.13 \phi_y \frac{d_b f_y}{\sqrt{f_c}} \quad 3.4$$

where ϕ_y is the yield curvature of the section, h is the section height, d_b is the longitudinal bar diameter, f_y and f_c are the resistance of steel and concrete in MPa, respectively, and L_V is the shear span (equal to the ratio between bending moment and shear). For columns, a double bending distribution is commonly assumed, and hence L_V is half of the interstorey height.

The yield curvature is calculated according to the relationship proposed by Priestley (1997):

$$\phi_y = 2.14 \frac{\varepsilon_y}{h} \quad 3.5$$

where ε_y is the yield strain of the longitudinal rebars.

- **Significant damage limit state (LS2):** The chord rotation capacity is limited to $\frac{3}{4}$ of the ultimate rotation capacity Θ_u (Panagiotakos and Fardis, 2001; CEN, 2003):

$$\Theta_u = \frac{1}{\gamma_{el}} \left[\Theta_y + (\phi_u - \phi_y) L_{pl} \left(1 - \frac{0.5L_{pl}}{L_v} \right) \right] \quad 3.6$$

where γ_{el} is 1,5 for the primary structural elements and 1 for all others, ϕ_u is the ultimate curvature and L_{pl} is the plastic hinge length. The plastic hinge length can be calculated as:

$$L_{pl} = 0.1L_v + 0.17h + 0.24 \frac{d_b f_y}{\sqrt{f_c}} \quad 3.7$$

Whilst the ultimate curvature is assumed to be:

$$\phi_u = \frac{\varepsilon_{cu} + \varepsilon_{su}}{h} \quad 3.8$$

where ε_{cu} and ε_{su} are the ultimate concrete and steel strains, respectively. Calvi (1999) suggested the following ranges for the ultimate strain capacity:

$\varepsilon_{cu} = 0,5\% - 1\%$; $\varepsilon_{su} = 1,5\% - 3\%$ for poorly confined RC element

$\varepsilon_{cu} = 1\% - 2\%$; $\varepsilon_{su} = 4\% - 6\%$ for well confined RC elements

- **Collapse limit condition:** The chord rotation capacity is limited to the ultimate rotation capacity Θ_u .

The displacement capacity for each LS of interest is the displacement at the centre of mass of the building, being defined on the basis of the limit conditions described in the previous section and the deformed shape associated to the failure mechanism. As discussed previously, the limit conditions are given in terms of chord rotations that, for columns, correspond to the interstorey drift. To define the displacement capacity on the pushover curve corresponding to the interstorey drift, the height of an equivalent SDOF system has to be evaluated. According to Priestley (1997), a coefficient κ_1 to be applied to the total building height is introduced:

$$\begin{aligned} k_1 &= 0.64 && \text{for } n \leq 4 \\ k_1 &= 0.64 - 0.0125(n - 4) && \text{for } 4 < n < 20 \\ k_1 &= 0.44 && \text{for } n \geq 20 \end{aligned} \quad 3.9$$

where n is the number of storeys of the building. Although the equations above refer to the global collapse mechanism activated at foundation level, in this application they have been considered adequate for other types of failure mechanism.

A linear deformed shape is assumed within the elastic range. Therefore, the displacement capacity associated to the light structural damage (LS1), which corresponds on the pushover curve to the yielding point, is given by:

$$\Delta_{SL1} = k_1 H_T \Theta_y \tag{3.10}$$

where H_T is the global building height.

In the post-elastic range the deformed shape is assumed as shown in Figure 3.7 for beam-sway and column-sway mechanisms. When the beam-sway collapse-mechanism is activated, the procedure accounts for the centre of mass moving up towards the centre of mass of the part of the building that is involved in the collapse mechanism. Hence, Eqs. 3.11 and 3.12 define the displacement capacity for global and soft storey failure mechanisms, respectively:

$$\Delta_{SLi} = \Delta_{LS1} \frac{H_k^*}{k_1 H_T} + (\Theta_{LSi} - \Theta_y) H_k \tag{3.11}$$

$$\Delta_{SLi} = \Delta_{LS1} + (\Theta_{LSi} - \Theta_y) h_p \tag{3.12}$$

where i is equal to 2 or 3 for the significant damage and collapse limit states, respectively, h_p is the inter storey height and H_k is the equivalent height of the part of the building above the activation of the global collapse failure mechanism and H_k^* is H_k plus the height to activation of the mechanism.

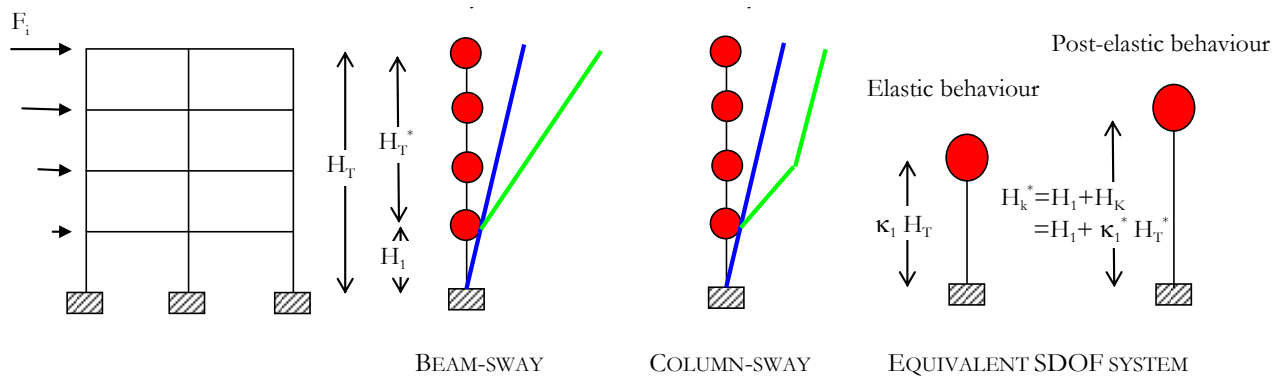


Figure 3.7. Deformed shape for (left) beam-sway and (right) column-sway collapse mechanisms activated above the first floor. The black line represents the elastic deformed shape and the grey line the post-yield mechanism.

An extensive validation exercise has been undertaken comparing the simplified pushover curve calculated in SP-BELA with the one obtained by refined non linear finite element analyses (Borzi, 2006). Some results are reported in Appendix A.

3.1.2 Masonry buildings

The simplified pushover curve adopted in SP-BELA to describe the capacity of masonry buildings has an elastic perfectly plastic behaviour. The pushover curve can describe the behaviour of masonry buildings that activate a global failure mechanism and do not fail as a consequence of out of plane local failure mechanisms (see Figure 3.8). For a general model aimed to the large scale vulnerability assessment it is difficult to take into account the out of plane failure mechanisms, because they are related to the peculiar condition of a building that are difficult to extend to others. Hence in SP-BELA a mechanic model is done to describe the behaviour of buildings that activate a global collapse failure mechanism, which can be identified as low vulnerability buildings, and the results of observations are integrated to account for out of plane failure mechanism and other high vulnerability conditions. Therefore, the SP-BELA approach for masonry buildings can be classified as hybrid since a mechanic model and the results of observations are both considered.

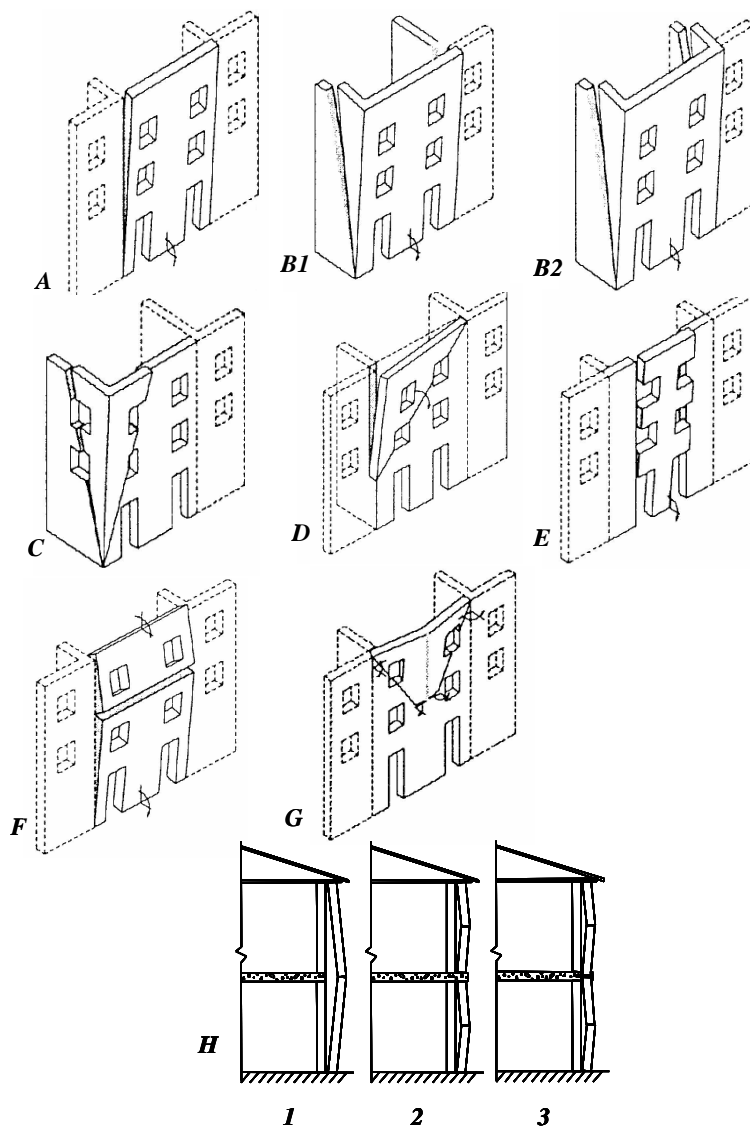


Figure 3.8. Types of out of plane collapse failure mechanisms (Restrepo-Velez and Magenes, 2004, adapted from D'Ayala and Speranza, 2003).

Low vulnerability buildings

A masonry wall is able to resist lateral in-plane forces with a combination of flexural, shear and rocking mechanisms. In general, in squat walls there will be a larger contribution of the shear mechanism, whereas in slender walls, flexural and rocking mechanisms will tend to be activated. A further classification of the shear failure mechanism can be made between the one that produces: diagonal cracks in the mortar around the bricks or across the bricks as a function of the relative resistance of the mortar and the bricks and horizontal cracks in the mortar along the bed joints. A valuable description of the aforementioned failure mechanisms is documented in Magenes et al. (2000) and Restrepo-Velez and Magenes (2004).

The analysis methodology proposed herein uses the definition of a single-degree-of-freedom system (SDOF system) which is equivalent to the original multi-degree-of-freedom system (MDOF system) in terms of mass, stiffness and displacement capacity. The original MDOF system has masses m_i that account for the mass of the floor slabs and masonry and is subjected to lateral forces F_i , which for masonry buildings with a number of floors less than 5 (upper bound in terms of number of storey as a consequence of the structural limits and bearing capacity of the material), can be assumed linearly distributed along the building height.

With the objective of defining the displacement capacity of the SDOF system, a deformed shape should be assumed for each limit state condition. Within the elastic range, a linear deformed shape is considered, whereas for post-yield limit states, a soft-storey mechanism is predicted (Calvi, 1999). Once the deformed shape has been assumed, the displacement capacity associated with the limit conditions is calculated for the drift values reported in the following:

- **Light damage limit state (LS1):** an average drift of 0.13% with a c.o.v. of 35% and a normal distribution can be used to identify the light damage limit condition (Abrams, 1997; Magenes et al., 1997; Calvi, 1999; Restrepo-Velez, 2003);
- **Significant damage limit state (LS2):** an average drift of 0.34% with a c.o.v. of 30% and a normal distribution can be used to identify the significant damage limit condition (Abrams, 1997; Magenes et al., 1997; Calvi, 1999; Restrepo-Velez, 2003);
- **Collapse limit condition (LS3):** on the basis of experimental test results, for brick masonry with a low percentage of voids (i.e. void percentage lower than 55%) that can identify low vulnerability masonry buildings, an average drift of 0.72% and a c.o.v. of 35%, with a normal distribution is considered (Anthoine et al. (1994); Bosiljkov et al. (2003)).

The displacement capacity of the SDOF system at the limit of elastic behaviour (LS1) is given by:

$$\Delta_y = k_1 h_T \delta_y \quad 3.13$$

where k_1 is the coefficient that is multiplied by h_T , the total building height, to obtain the equivalent height of the SDOF system and δ_y is the drift at the limit of elastic behaviour (Restrepo-Velez and Magenes, 2004). If the building has a regular distribution of masses along the height k_1 is approximately 0.67.

As a consequence of the assumption of a soft-storey mechanism, the plastic deformations are concentrated within the height h_p , which is considered herein to correspond to the interstorey height. For buildings with a large number of openings, the soft-storey mechanism should develop over a height that is greater than the opening height and less than the interstorey height. In this case, the use of the interstorey height would not be conservative as it would increase the building displacement capacity. This assumption is, however, acceptable because it compensates for the conservative assumptions that are typical within a mechanics-based vulnerability method where many contributions to the structural building resistance (e.g. contribution of partition walls) are

neglected. Therefore, the displacement capacity for the limit states corresponding to a structure entering the non-linear range is:

$$\Delta_{LSi} = k_1 h_T \delta_y + k_2 (\delta_{LSi} - \delta_y) h_p \tag{3.14}$$

where δ_{LSi} is the drift limit state capacity corresponding to severe damage and collapse limit condition.

For the evaluation of displacement capacity in the equations above, the coefficients k_1 and k_2 need to be defined. For masses uniformly distributed along the building height and for walls with a mass equal to 30% of the floor mass, Restrepo-Velez (2003) has calculated k_1 and k_2 , as summarised in Table 3.1. These values are valid for the cases where collapse mechanisms are activated within the first 2/3 of the building height.

Table 3.1. k_1 and k_2 coefficients as a function of number of floors (Restrepo-Velez, 2003).

Number of Floors	k_1	k_2
1	0.790	0.967
2	0.718	0.950
3	0.698	0.918
4	0.689	0.916
5	0.684	0.900
6	0.681	0.881

Once the displacement capacity has been defined, in order to fully describe the pushover curve the collapse multipliers have to be calculated. As suggested by Restrepo-Velez and Magenes (2004), the formula given by Benedetti and Petrini (1984) can be used for the collapse multiplier λ_i at the interstorey i :

$$\lambda^i = \frac{1}{\frac{\sum_{k=1}^n h_k W_k}{W_T} \frac{\sum_{j=1}^n h_j W_j}{W_T}} A_i \tau_{ki} \left[1 + \frac{\sum_{k=1}^n W_k}{1.5 \tau_{ki} A_i (1 + \gamma_{AB})} \right]^{1/2} \tag{3.15}$$

where:

- W_T is the total weight of the building;
- W_i is the weight of the floor i ;
- τ_{ki} is the shear resistance of the masonry at floor i ;
- A_i is the total area of resisting walls at level i in the direction of application of loads;
- γ_{AB} is the ratio between A_i and B_i with B_i being the maximum area between the area of wall in the loaded direction and the orthogonal direction;

- n is the number of storeys.

The building collapse multiplier will be the smallest amongst all of the calculated λ^i :

$$\lambda = \min\{\lambda^i\} \quad 3.16$$

The formula of λ^i given by Benedetti and Petrini (1984) neglects 3D effects such as torsion due to an eccentricity between the centre of stiffness and the centre of mass of the building. Restrepo-Velez and Magenes (2004) have therefore suggested the introduction of a correction coefficient expressed by:

$$\lambda = \phi_c^{-1} \min\{\lambda^i\} \quad 3.17$$

The correction coefficient ϕ_c has been defined through comparison with results of finite element analyses on 3D buildings with the code SAM (Simplified Analysis of Masonry) that has been developed and verified by Magenes and Della Fontana (1998) and Magenes et al. (2000), amongst others. Through a regression analysis on the obtained results, the following formulation of ϕ_c has been obtained by Restrepo-Velez and Magenes (2004):

$$\phi_c = 5.5 \frac{\tau_{ki}}{\frac{L_W}{L_T}} + 0.5 \quad 3.18$$

where L_T is the total length of the walls in the direction of loads and L_W is the total length of the walls without openings in the loaded direction.

Average and high vulnerability masonry buildings

As a function of their vulnerability, masonry buildings have been classified in the technical literature into three vulnerability classes (Braga et al., 1982): class A (high vulnerability), B (average vulnerability) and C (low vulnerability). As already stated, the SP-BELA method does not provide building capacity for highly vulnerable masonry buildings due to the lack of data necessary for the description of the sample since there are several mechanisms which characterise the high vulnerability and no data are available to describe all the building samples needed. To take into account highly vulnerable masonry buildings a hybrid method has been adopted. Such method uses SP-BELA, but it also integrates the damage observations of past earthquakes. Such data have been organised in damage probability matrices (DPM) that indicate, for each vulnerability class, the percentage of damaged buildings corresponding to each seismic intensity considered.

Observed damage data herein included are the one summarised in the damage probability matrix published in Braga et al. (1982). Such matrix come from a statistic of post-event data collected in the municipalities affected by the 1980 Irpinia earthquake. The hazard is expressed in MKS macroseismic intensity scale (Medvedev Sponheuer Scale, 1969). The DPMs consider 5 damage levels, besides the absence of damage.

The information contained in the matrices were used to produce fragility curves, an alternative way to represent the probability of reaching or exceeding a certain damage limit condition. Then the multiplicative coefficients have been calculated, that allow to obtain, for each limit state, the fragility curves for the class A and B starting from the curve for the class C. The use of these coefficients acquires significance if it is assumed that passing from a class of vulnerability to the other the dispersion value of the fragility curve is preserved and the quality of

the masonry affects only the average value of the curve. The first step was to find a correspondence between the levels of damage taken into account in the DPM and the SP-BELA limit states. It was assumed that: the damage levels 1 and 2 correspond to light damage, the level 3 corresponds to significant damage and levels 4 and 5 correspond to collapse. The DPMs developed by Braga et al. (1982) were used to understand the relationship in terms of probability of damage between the three classes of masonry. Fragility curves have been defined through the best fit with a lognormal curves between the point corresponding to the damage probability matrix. Hence the assumption that the fragility curves corresponding to the different vulnerability classes are characterised by a different average and by the same dispersion parameter (i.e. the same CV) is undertaken.

Once this correspondence was established, the fragility curves for points obtained from the DPM were plotted and then interpolated using a lognormal function in order to obtain continuous curves. Figure 3.9 shows the curves for the limit state of significant damage. In the aforementioned figure a continuous line plots the curves resulting from the discrete DPM developed by Braga et al. (1982), while the dashed lines plots the lognormal best fit curves which best interpolates them. The good correspondence between the curves demonstrates that the lognormal distribution is a good mathematical function to describe the probability distribution of damage data coming from observations.

The next step was to control whether, for each limit state, starting from the lognormal curve obtained by interpolating the points of the damage probability matrix for the vulnerability class C, it was possible to obtain the fragility curves for the other two classes of vulnerability. For each limit state the ratio between the mean value of the curve for class C and the mean of the curves for class A and B was calculated. These ratios are the desired coefficients reported in Table 3.2 as a function of the limit state. Then the coefficient of variation CV of the curve for class C ($CV = \text{ratio between the standard deviation and the mean value of the curve}$) was calculated and it was made the hypothesis that the fragility curves for the class of vulnerability A and B have different mean value, but the same CV of the curve for class C, assuming that the dispersion is the same. To validate this hypothesis, Figure 3.10 shows the comparison between the fragility curves for classes A and B obtained by interpolating the corresponding DPM (dashed line) and the fragility curves obtained starting from the curve for class C and modifying the average value using the coefficients shown in Table 3.2 (continuous line) for the significant damage limit state. Curves obtained from the curve for class A and B well approximate those derived by the interpolation of the DPM.

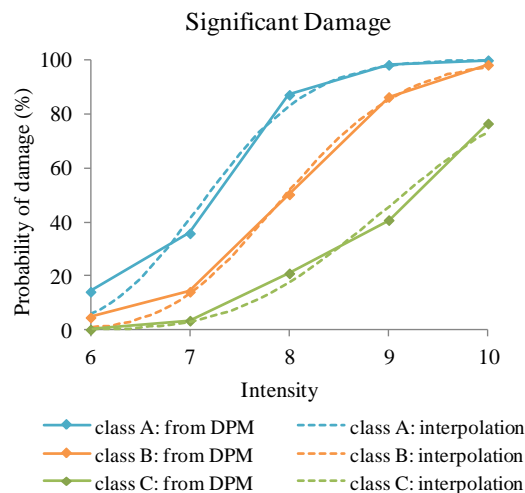


Figure 3.9. Fragility curves obtained from DPM developed by Braga et al. (17) and lognormal function which best interpolates them.

Table 3.2. Multiplicative coefficients that allow to obtain, for each limit state, the fragility curves for the class A and B starting from the curve for the class C.

Limit state	Vulnerability class	
	A	B
Light damage	1.36	1.17
Significant damage	1.28	1.16
Collapse	1.26	1.15

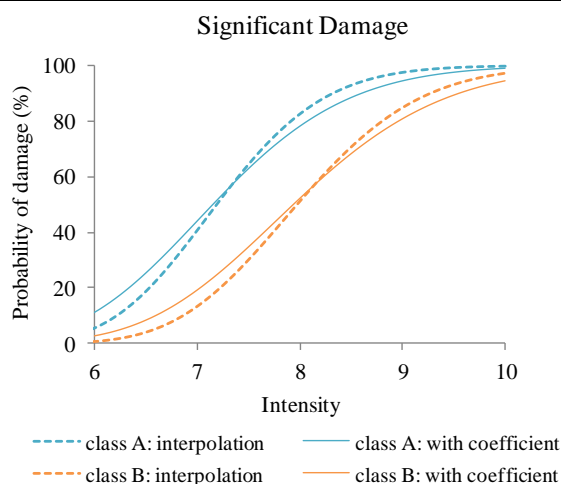


Figure 3.10. Fragility curves obtained by interpolating the corresponding DPM of Braga et al. (17) and curves obtained with the calculated coefficients.

Hence, SP-BELA could be adopted to calculate fragility curves for the vulnerability class C and then those for classes A and B were obtained using the coefficients summarised in Table 3.2.

However, the approach herein presented does not use fragility curves to compute the risk, because the capacity is defined for the building sample through pushover curves then compared with the demand imposed by the ground shaking. If the demand is higher than the capacity the building does not survive the damage limit condition and evolve to a higher damage. In Figure 3.11 the green dots represent those buildings that satisfy the limit condition, while the red ones represent the buildings that fail the limit condition and hence will evolve to the next damage level.

Analysing the results of such a comparison in a statistical framework, the risk is computed as conditional failure probability:

$$P_{ik} = P[D \geq d_i \mid E = e_k] \quad 3.19$$

where d_i is the damage limit condition and e_k is the ground shaking severity parameter.

Such an approach corresponds to calculate 1 point of the fragility curves. As a consequence the coefficients of Table 3.2 are used to increase the input ground shaking instead of reducing the average value of the fragility curves leading to results that numerically match.

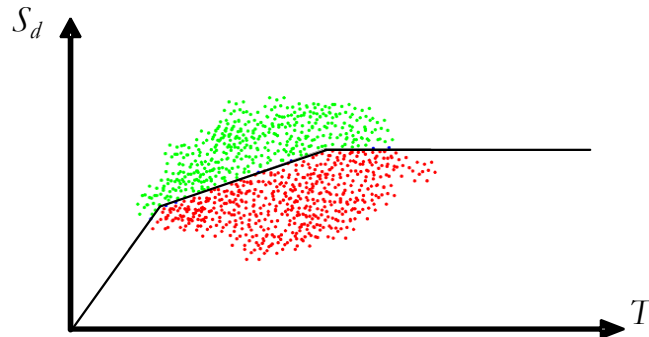


Figure 3.11. Comparison between capacity and demand on the plane of displacement spectrum. Each dot represents a building of the sample.

4 PROPOSED METHOD TO ACCOUNT FOR PROGRESSIVE DAMAGE

4.1 MODIFICATIONS OF SP-BELA TO ACCOUNT FOR PROGRESSIVE DAMAGE

The SP-BELA method is applied to define the building capacity without computing the fragility curves, as mentioned previously in the current document. This choice has two main advantages for the applications within the NERA project that are:

1. evaluating the probability of reaching or exceeding a damage limit conditions through a comparison between displacement demand and capacity (see **Figure 3.11**), the effects of the frequency content of the ground shaking can be explicitly taken into account. The alternative could be to compute the fragility curve as a function and a ground shaking parameter (e.g., PGA) anchoring to each point of the abscise of the curve a spectral shape. Such a shape does not match to the one corresponding to the earthquake that shall be considered to calculate the seismic risk;
2. the effect of progressive damage can be computed modifying directly the capacity curve.

In order to account for the progressive damage, the FEMA coefficients for bare frame, frame with infill wall and masonry panels are taken into account. Such coefficients are summarised in Table 4.1, Table 4.2 and

Table 4.3.

Table 4.1. FEMA coefficients for RC bare frame.

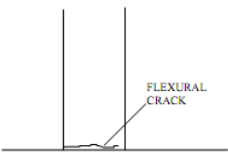
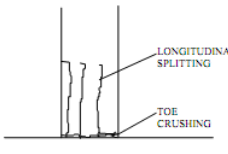
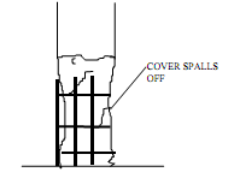
Severity	Coefficients	Damage
Insignificant	$\lambda_K = 0.9$ $\lambda_Q = 1.0$ $\lambda_D = 1.0$	 <p>FLEXURAL CRACK</p>
Moderate	$\lambda_K = 0.8$ $\lambda_Q = 0.5$ $\lambda_D = 1.0$	 <p>LONGITUDINAL SPLITTING TOE CRUSHING</p>
Heavy	$\lambda_K = 0.5$ $\lambda_Q = 0.5$ $\lambda_D = 1.0$	 <p>COVER SPALLS OFF</p>

Table 4.2. FEMA coefficients for RC frame with infill walls.

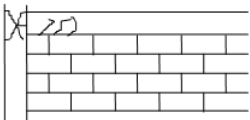
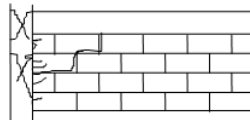
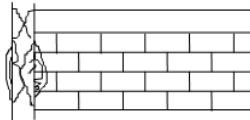
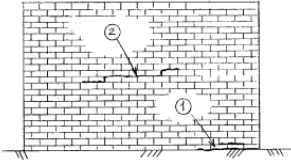
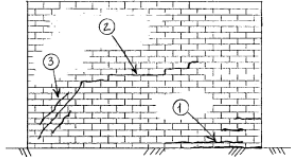
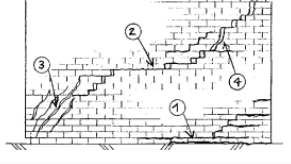
Severity	Coefficients	Damage
Insignificant	$\lambda_K = 0.9$ $\lambda_Q = 0.9$ $\lambda_D = 1.0$	
Moderate	$\lambda_K = 0.7$ $\lambda_Q = 0.7$ $\lambda_D = 0.4$	
Heavy	$\lambda_K = 0.4$ $\lambda_Q = 0.2$ $\lambda_D = 0.4$	

Table 4.3. FEMA coefficients for masonry wall.

Severity	Coefficients	Damage
Insignificant	$\lambda_K = 0.9$ $\lambda_Q = 1.0$ $\lambda_D = 1.0$ $\mu_{\Delta} \leq 1.5$	
Heavy	$\lambda_K = 0.8$ $\lambda_Q = 0.8$ $\lambda_D = 1.0$ $\Delta/heff \leq 0.3\%$	
Extreme	$\lambda_K = 0.6$ $\lambda_Q = 0.6$ $\lambda_D = 0.9$ $\Delta/heff \leq 0.9\%$	

The coefficients applied to the pushover curves are linearly interpolated between light damage and collapse limit conditions as a function of the performance point corresponding to the previous shaking. The pushover curve is not modified if the building does not exceed the light damage limit condition.

The SP-BELA routine has been modified in order to be used to assess the progressive damage of buildings during a seismic sequence, assuming that both simulated data of ground motion and actual spectra derived for a real aftershock will be available. The flow chart of the procedure is shown in Figure 4.1. At the start the pushover curves of the undamaged building is computed. Hence two different paths can be followed:

- if the simulated hazard is used as an input, then the risk is calculated but the pushover curves are not updated, since a further shaking did not really occur;
- if the ground shaking scenario is real, i.e. a real aftershock has occurred, then the risk is computed and, as a function of the performance point reached by each building, the properties of the pushover curve are updated.

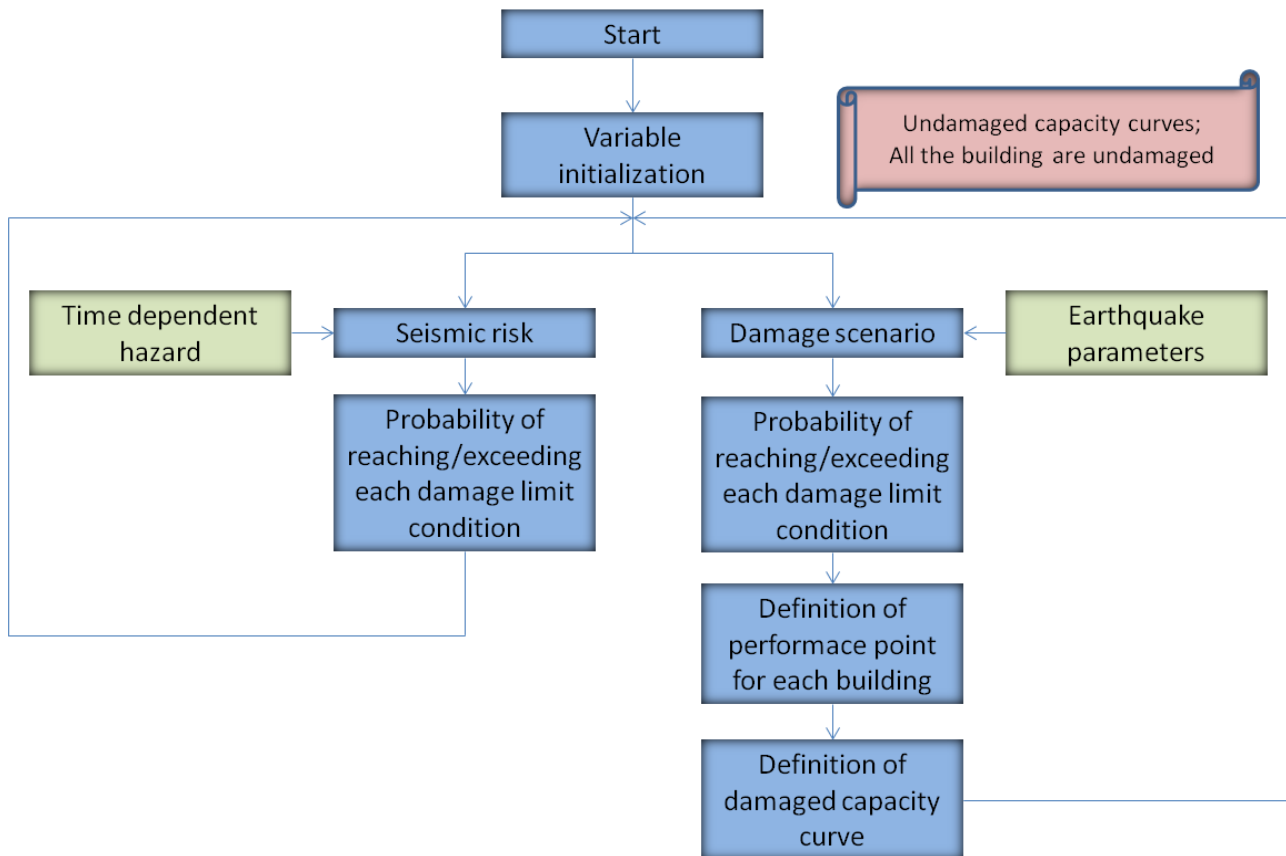


Figure 4.1. Workflow of the procedure to account for progressive damage.

The full implementation of the procedure for real time damage assessment will be described in the deliverable D14.3, while an example of the results of the proposed procedure on a 3 storey masonry building is showed in the following.

4.1.1 Application of the SP-BELA method accounting for progressive damage

A three storey masonry building has been subjected 3 times to the same ground shaking. The elastic displacement spectrum of the ground motion is shown in Figure 4.2.

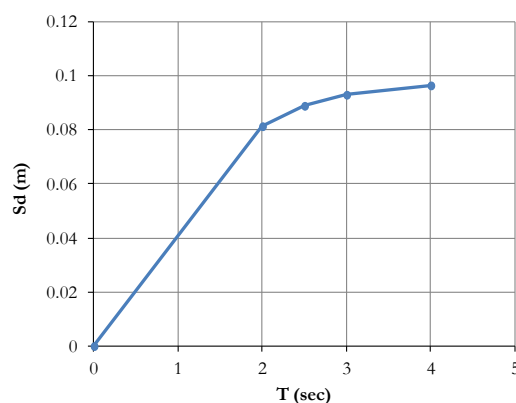


Figure 4.2. Elastic displacement spectrum of the selected ground shaking.

The comparison between capacity and demand imposed on the building by the ground shaking is shown in Figure 4.3 on the plan of inelastic spectral displacement and spectral acceleration. When the earthquake hit the undamaged building the performance point lays between LS1 and LS2 (see Figure 4.3a). At the second shaking the performance point is almost corresponding to LS2 (see Figure 4.3b). At the third time the performance point is placed between LS2 and LS3 (see Figure 4.3c). Therefore, although the ground shaking is kept constant, as a consequence of progressive damage the building evolves toward collapse.

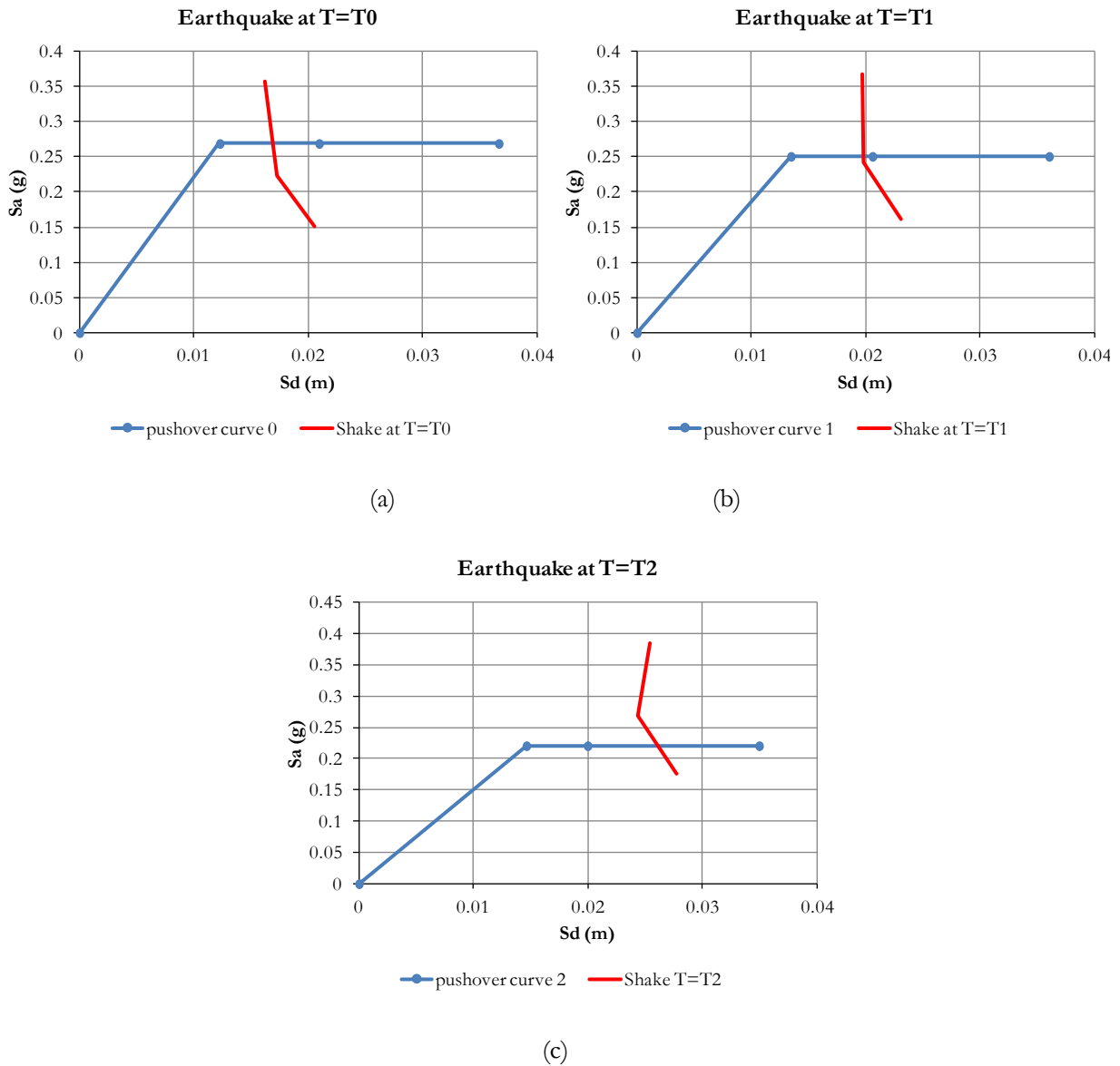


Figure 4.3. Comparison between capacity and demand for the performance point definition.

In order to highlight the influence of progressive damage, the pushover curve of the building after each of the aforementioned ground shaking is shown in Figure 4.4.

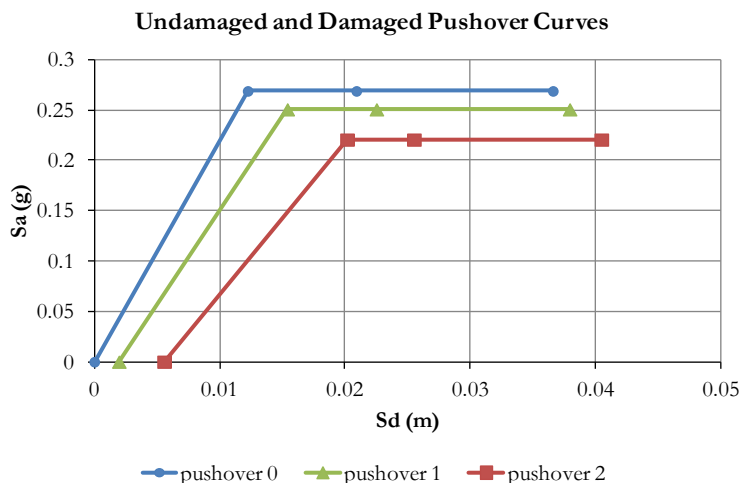


Figure 4.4. Pushover curve of a 3 storey masonry building after three ground shaking hitting in progression the building.

Finally, in Figure 4.5 the probability of reaching or exceeding the three limit conditions for a population of 3 storey masonry buildings at each of the aforementioned ground shaking is represented. The trend observed for a single building can be seen also in probabilistic terms considering a building population. After each ground shaking, although level of shaking is kept constant, the probability of accumulating damage increases (i.e., the probability of exceeding LS2, severe damage, and LS3, collapse).

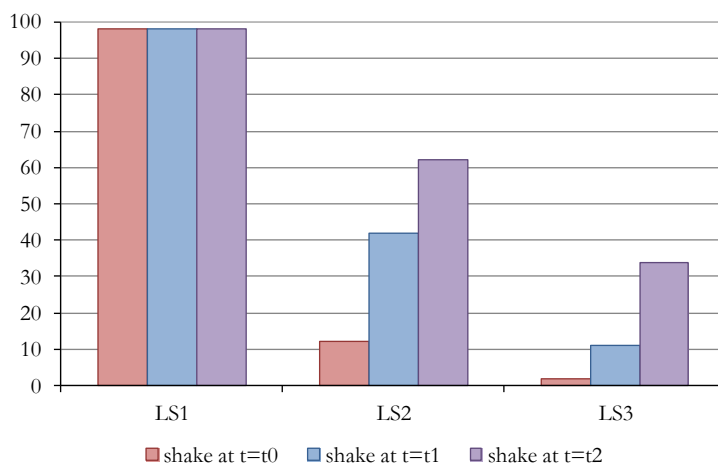


Figure 4.5. Probability of reaching or exceeding the damage limit conditions at each of the three repetitions of the considered ground shaking.

5 CLOSURE AND FURTHER DEVELOPMENTS

The FEMA coefficients should be toned and validated. One way to do this is to start an analysis campaign. A first attempt has been made in order to measure the effects of progressive damage of the initial stiffness on RC bare frame (Miglietta et al., 2012), but further analyses are needed for all the other parameters (e.g., base shear resistance, displacement capacity) and all the other structural types. The results of this investigation have been published in Miglietta et al (2012).

The work described in this report will be integrated within the general hazard and risk framework as currently being discussed within NERA.

REFERENCES

- Abrams D.P. (1997) "Response of unreinforced masonry buildings", *Journal of Earthquake Engineering*, Vol. 1, No. 1, pp. 257-273.
- Anthoine A., Magenes G. and Magonette G. (1994) "Shear compression testing and analysis of brick masonry walls", In *Proceedings of the 10th World Conference on Earthquake Engineering*, Vienna.
- Benedetti D. and Petrini V. (1984) "Sulla vulnerabilità sismica di edifici in muratura: Proposta su un metodo di valutazione", *L'industria delle Costruzioni*, Vol. 149, pp. 66-74 (in Italian).
- Bolognini D., Borzi B., Pinho R. (2008) "Simplified Pushover-Based Vulnerability Analysis of Traditional Italian RC Precast Structures", *Proceeding of 14th World Conference on Earthquake Engineering*, Beijing 2008.
- Borzi B. (2006) "Validazione della metodologia semplificata per l'esecuzione di analisi pushover", *Rapporto di Ricerca*. European Centre for Training and Research in Earthquake Engineering (EUCENTRE), Pavia, Italia.
- Borzi B., Pinho R., Crowley H. (2007) "Simplified Pushover-Based Vulnerability Analysis for Large Scale Assessment of RC Buildings", *Engineering Structures*, Vol. 30, No. 3, pp. 804-820.
- Borzi B., Crowley H., Pinho R. (2008) "Simplified Pushover-Based Earthquake Loss Assessment (SP-BELA) Method for Masonry Buildings", *International Journal of Architectural Heritage*, Vol. 2, No. 4, pp. 353-376.
- Braga F., Dolce M., Liberatore D. (1982) "A statistical Study on damage buildings and an ensuing review of the M.S.K. – 76 scale", *Atti del 7 ECEE*, Atene.
- Calvi G.M. (1999) "A displacement-based approach for vulnerability evaluation of classes of buildings", *Journal of Earthquake Engineering*, Vol. 3, No. 3, pp. 411-438.
- CEN - Comité Européen de Normalisation (2003) "prEN 1998-1-Eurocode 8: design of structures for earthquake resistance – Part 1: General rules, seismic actions and rules for buildings", Brussels.
- Cosenza E., Manfredi G., Polese M., Verderame G.M. (2005) "A multi-level approach to the capacity assessment of existing RC buildings", *Journal of Earthquake Engineering*, Vol. 9, No.1, pp. 1-22.
- D'Ayala D. and Speranza E. (2003) "Definition of collapse mechanisms and seismic vulnerability of masonry structures", *Earthquake Spectra*, Vol. 19, No. 3, pp. 479-509.
- Dolsek M., Fajfar P. (2004) "IN2- A simple alternative for IDA", *13th World Conference on Earthquake Engineering*. Vancouver, B.C., Canada. Paper No. 3353.
- Federal Emergency Management Agency 273 (1997) "NEHRP Guidelines for the Seismic Rehabilitation of Buildings", Washington DC.
- Federal Emergency Management Agency 306 (1998) "Evaluation of Earthquake Damaged Concrete and Masonry Wall Buildings - Basic Procedures Manual", Washington DC.
- Federal Emergency Management Agency 307. (1998) "Evaluation of Earthquake Damaged Concrete and Masonry Wall Buildings - Technical Resources", Washington DC.

Magenes G., Kingsley G.R. and Calvi G.M. (1997) “Seismic testing of a full-scale, two-story masonry building: Test procedure and measure experimental response”, Gruppo Nazionale per la Difesa dai Terremoti.

Magenes G., Della Fontana A. (1998) “Simplified non-linear seismic analysis of masonry buildings”, Proceedings of the British Masonry Society, Vol. 8, pp. 190-195.

Magenes G., Bolognini D. and Baggio C. (2000) “Metodi semplificati per l’analisi sismica non lineare di edifici in muratura”, CNR-Gruppo Nazionale per la Difesa dai Terremoti, Roma, 99 pp., http://gndt.ingv.it/Pubblicazioni/Magenes_copertina_con_intestazione.htm (in Italian).

Mainstone R.J. (1971) “On the stiffness and strength of infilled frames”, Proceedings of the Institution of Civil Engineers, Supplement IV, 57-90.

Masi A. (2004) “Seismic Vulnerability Assessment of Gravity Load Designed R/C Frames”, Bulletin of Earthquake Engineering, Vol. 1, No.3, 371-395.

Medvedev A.V, Sponheuer W. (1969) “Scale of seismic intensity”, Proceeding of The 4th World Conference on Earthquake Engineering. Santiago del Cile, Cile.

Miglietta P., Ceresa P., Iaccino R., Borzi B. (2012) “Accounting for progressive damage in large scale seismic risk assessment of RC buildings”, Proceedings of 15th Word Conference on Earthquake Engineering, Lisbon, Paper N. 5173. ISBN 978-989-20-3182-8.

Panagiotakos T., Fardis M.N. (2001) “Deformation of r.c. members at yielding and ultimate”, ACI Structural Journal, Vol. 98, pp. 135-148.

Polese M., Di Ludovico M., Prota A., Manfredi G. (2012) “Damage-depent vulnerability curves for existing buildings”, Earthquake Engineering Structural Dynamics, published online in Wiley Online Library, DOI: 10.1002/eqe.2249.

Priestley M.J.N. (1997) “Displacement-based seismic assessment of reinforced concrete buildings”, Journal of Earthquake Engineering, Vol 1, pp. 157-192.

Restrepo-Vélez, L.F. (2003) “A simplified mechanics-based procedure for the seismic risk assessment of unreinforced masonry buildings”, Individual Study, ROSE School, Pavia, Italy.

Restrepo-Vélez, L.F. and Magenes, G. (2004) “Simplified procedure for the seismic risk assessment of unreinforced masonry buildings”, Proceedings of the Thirteenth World Conference on Earthquake Engineering, Vancouver, Canada, Paper no. 2561.

Rota M., Penna A., Magenes G. (2010) “A methodology for deriving analytical fragility curves for masonry buildings based on stochastic nonlinear analyses”, Engineering Structures, 32: 1312-1323.

Singhal A., Kiremidjian A.S. (1996) “Method for probabilistic evaluation of seismic structural damage”, Journal of Structural Engineering, ASCE, Vol. 122, No. 12, pp. 1459-1467.

APPENDIX A

VALIDATION OF SIMPLIFIED METHODOLOGY TO CALCULATE THE PUSHOVER CURVE FOR RC FRAME BUILDINGS IN SP-BELA

In order to assess the adequacy of the proposed procedure in the computation of simplified pushover curves, comparisons with results obtained from Finite Element (FE) analyses have been carried out. The latter have been conducted with SeismoStruct (SeismoSoft, 2006), a fibre-element based program for seismic analysis of framed structures, which can be freely downloaded from the Internet. The program is capable of predicting the large displacement behaviour and the collapse load of framed structures under static or dynamic loading, duly accounting for geometric nonlinearities and material inelasticity. Its accuracy in predicting the seismic response of reinforced concrete structures has been demonstrated through comparisons with experimental results derived from pseudo-dynamic tests carried out on large-scale models (e.g. López-Menjivar, 2004; Casarotti and Pinho, 2006).

A 4-storey building designed according to the 1992 Italian design code (DM, 1992), considering gravity loads only, and the Decreto Ministeriale 1996 (DM, 1996), considering a seismic load equal to 10% of the seismic weight, have been used in this brief validation study. The possibility of both regularly and irregularly (pilotis) distributed infill panels with height is also taken into account. The building has the same plan as that shown in Figure 3.2. The span dimensions in the x and y directions are 5 m and 6 m, respectively. It has been loaded with a triangular distribution of lateral forces, and the collapse multiplier λ and the displacement capacity at the three limit states have been computed as described in Chapter 3. In the FE model the panels are represented by strut elements with a softening behaviour after the yield limit condition corresponding to a compression stress equal to 1.2 MPa. A very low residual resistance has been taken into account only to guarantee the numerical stability of the model.

Figure A1 shows the comparison between the simplified and the FE analyses for lateral forces applied along the x and y direction of the RC building designed only considering gravity loads. For the configuration with regularly distributed infill panels, both the FE analysis and the simplified method (SP-BELA) predict the activation of a soft-storey mechanism at the 3rd storey and a global mechanism at the 3rd floor for the x and y directions, respectively. For the non-seismically designed pilotis building, the simplified analysis predicts an average situation between a soft-storey and global mechanism, because the external frames have weaker columns than beams whilst the inner frames have stronger columns than beams; on the other hand, a global failure mechanism is detected in the FE analysis. In the y-direction a global mechanism is predicted by both the simplified and more rigorous nonlinear analysis. In both directions, the comparison in terms of pushover curves is satisfactory, as can be seen Figure A2.

The case of buildings designed accounting for lateral forces (i.e. seismically designed) is shown in Figure A3 and Figure A4 for regularly and irregularly distributed infill panels, respectively. In the case of regularly distributed panels, the building is expected to collapse according to a global mechanism activated at the first storey, whereas with the irregular distribution a soft-storey mechanism is activated at the first storey. In both cases shown in Figure A3 and in Figure A4 the same kind of mechanism is expected to be activated in the x and y direction and the results of the FE nonlinear analyses confirm the results of the simplified analysis in terms of prediction of the failure mechanism. Also, the comparison in terms of pushover curves can be considered satisfactory.

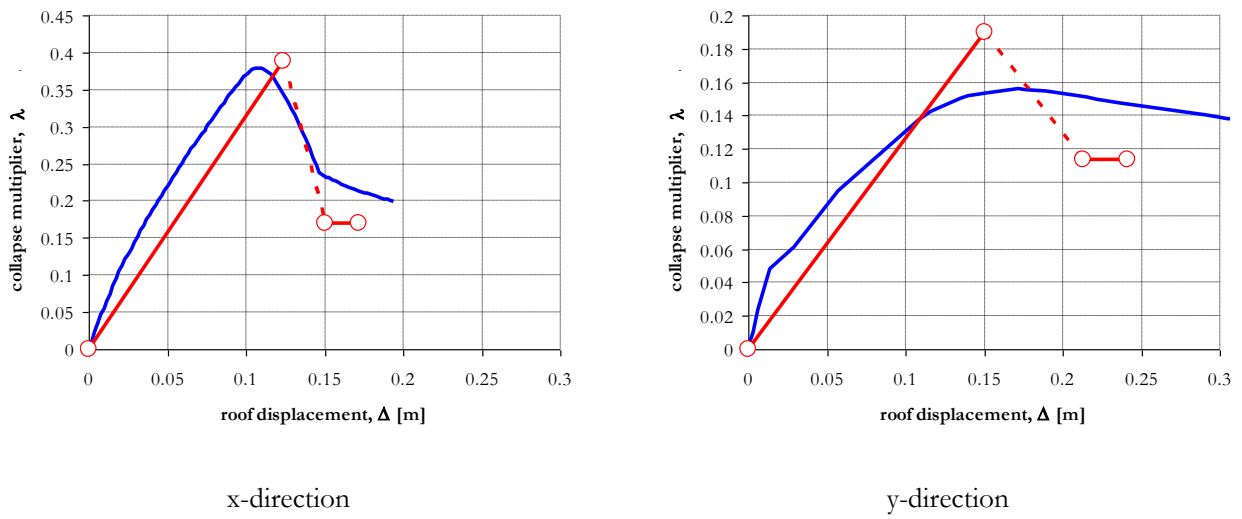


Figure A1 Comparison between pushover curves defined according to rigorous FE analysis (blue curve) and simplified analysis (red curve) for the case of non-seismically designed buildings with regularly distributed panels along the building height.

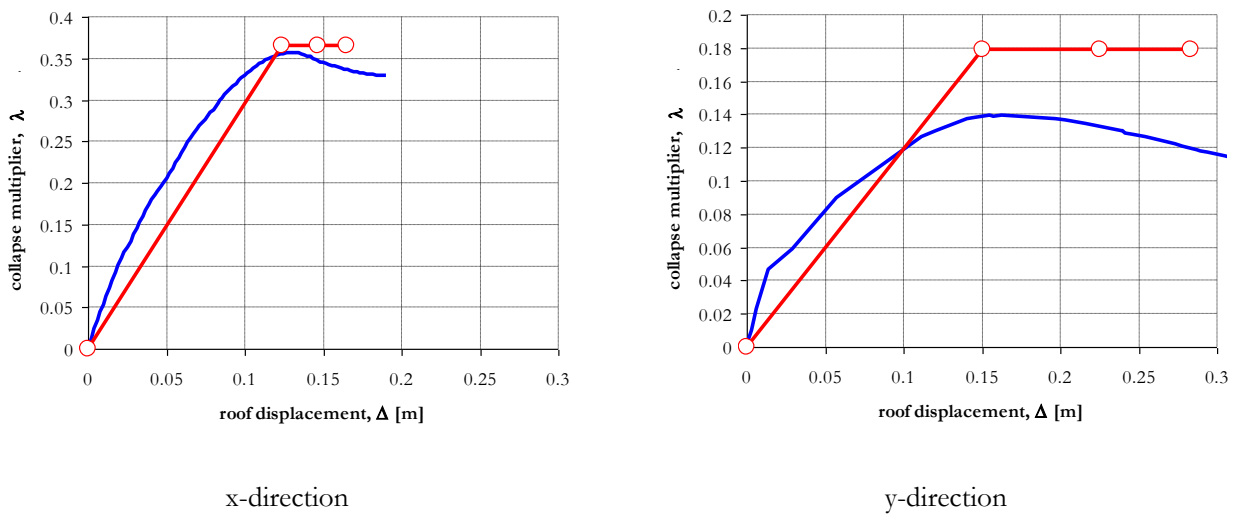
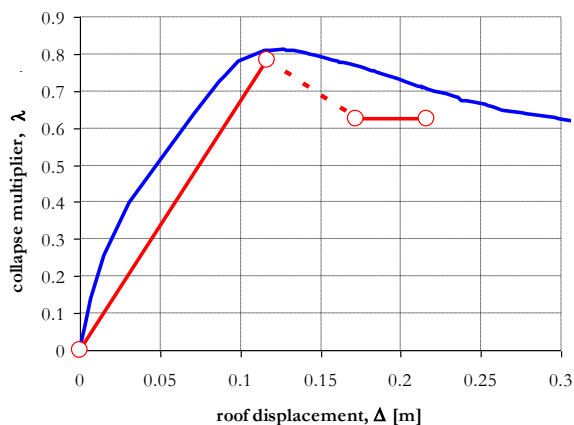
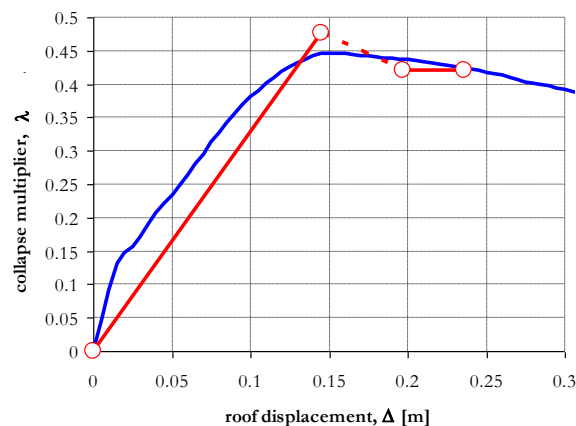


Figure A2 Comparison between pushover curves defined according to rigorous FE analysis (blue curve) and simplified analysis (red curve) for the case of non-seismically designed buildings with irregularly distributed panels along the building height (pilotis).

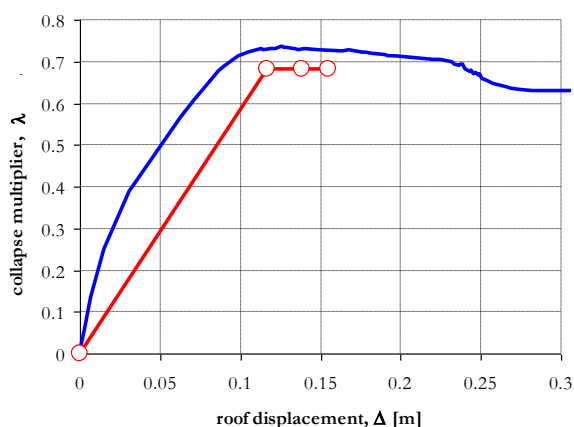


x-direction

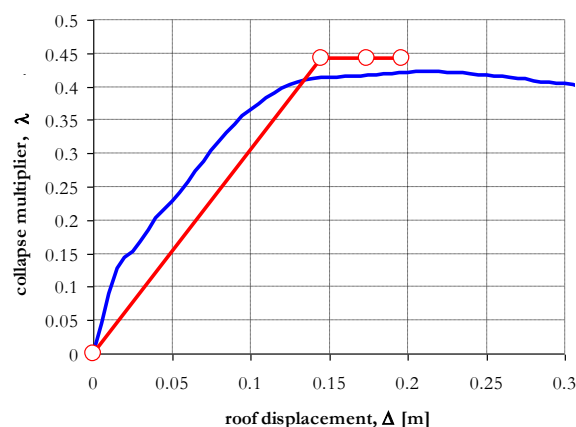


y-direction

Figure A3 Comparison between pushover curves defined according to rigorous FE analysis (blue curve) and simplified analysis (red curve) for the case of seismically designed buildings (seismic design force, c , equal to 10% of the seismic weight) with regularly distributed panels along the building height.



x-direction



y-direction

Figure A4 Comparison between pushover curves defined according to rigorous FE analysis (blue curve) and simplified analysis (red curve) for the case of seismically designed buildings (seismic design force, c , equal to 10% of seismic weight) with irregularly distributed panels along the building height (pilotis).

Hence, it is possible to state that the simplified procedure is able to capture the collapse multiplier and in most cases to predict the failure mechanism. Some differences might be observed in cases in which the simplified analyses predict a failure mechanism which is a mixture between the soft-storey and global failure, because some columns are more resistant than the connected beams and vice versa. In any case, in general, a good correspondence between the approximate and accurate pushover curve has been observed.

REFERENCES

SeismoSoft (2006) “SeismoStruct – A computer program for static and dynamic analysis for framed structures”, (online) Available from URL: www.seismosoft.com.

López-Menjívar M.A. (2004) “Verification of a displacement-based Adaptive Pushover method for assessment of 2-D Reinforced Concrete Buildings”, PhD Thesis, European School for Advances Studies in Reduction of Seismic Risk (ROSE School), University of Pavia, Italy.

Casarotti C. and Pinho R. (2006) “Seismic response of continuous span bridges through fibre-based finite element analysis”, *Journal of Earthquake Engineering and Engineering Vibration*, 5:1, 119-131

DM 92 (1992) “Norme tecniche per l'esecuzione delle opere in cemento armato normale e precompresso e per le strutture metalliche”, Decreto Ministeriale del 14 Febbraio 1992, pubblicato sulla *Gazzetta Ufficiale* n.65 del 18 marzo 1992 - Supplemento Ordinario n. 55.

DM 96 (1996) “Norme tecniche per le costruzioni in zone sismiche”, Decreto Ministeriale del 16 Gennaio 1996, pubblicato sulla *Gazzetta Ufficiale* n. 29 del 5 febbraio 1996.